Electrical Power and Energy Systems 148 (2023) 108906

Contents lists available at ScienceDirect

International Journal of Electrical Power and Energy Systems

journal homepage: www.elsevier.com/locate/ijepes

Integrating artificial neural networks and cellular automata model for spatial-temporal load forecasting

S. Zambrano-Asanza [a,b,*], R.E. Morales [c], Joel A. Montalvan [c], John F. Franco [a,d]

[a] Department of Electrical Engineering, São Paulo State University – UNESP, Ilha Solteira, SP, Brazil
[b] Department of Planning, CENTROSUR Electric Distribution Utility, Cuenca, Ecuador
[c] School of Electrical Engineering, University of Cuenca, Cuenca, Ecuador
[d] School of Energy Engineering, São Paulo State University – UNESP, Rosana, Brazil

ARTICLE INFO

Keywords:
Artificial neural network
Big data analytic
Cellular automata
Distribution planning
Geospatial analysis
Spatial load forecasting

ABSTRACT

The long-term distribution planning should include an understanding of consumer behavior and needs to develop strategic expansion alternatives that meet the future demand. The magnitude of growth along with the place where and when it will be developed are determined by the spatial load forecasting. Thus, this paper proposes a spatial-temporal load forecasting method to recognize and predict development patterns using historical dynamics and determine the development of consumers and electric load in small areas. An artificial neural network is integrated to a cellular automaton method to establish transition rules, based on land-use preferences, neighborhood states, spatial constraints, and a stochastic disturbance. The main feature is the incorporation of temporality, as well as taking advantage of geospatial-temporal data analytics to calibrate and validate a holistic and integral framework. Validation consists of measuring the spatial error pattern during the training and testing phase. The performance of the method is assessed in the service area of an Ecuadorian power utility. The knowledge extraction from large-scale data, evaluating the sensitivity of parameters and spatial resolution was carried out in reasonable times. It is concluded that adequate normalization and use of temporality in the spatial factors improve the error in the spatial-temporal load forecasting.

1. Introduction

Load forecasting is a fundamental input for the effective expansion planning of electrical distribution systems [1]. The future of electric demand along with the place where and when it will be developed is determined by spatial load forecasting (SLF). The planning process and SLF should incorporate a deep understanding of consumer behavior and needs to consider the impact on the performance of the electric power supply system [2,3]. Electrification is key to a clean, reliable and secure energy future, where new end-use technologies and high-consumption loads are being deployed in distribution networks, changing the seasonal load profiles of many utilities [4].

1.1. Previous work

Simulation methods project future consumer locations using location preference patterns to forecast where different "land uses" will be developed [5,6]. The location of consumers within a city depends on different needs, values, and behaviors; such patterns can be predictable [5]. For instance, the data mining technique, based on a "Knowledge Discovery in Database" procedure, automatically determines the preferential "scores" of land use changes [7].

To capture the influence of spatial factors on load growth patterns, a fuzzy inference model over a geographic information system (GIS) is presented in [8], thus obtaining a map of the potential for development. Each type of consumer in the map is associated with a saturation curve (S shape), as a function of time. In addition, cellular automata (CA) were

Abbreviations: ANN, Artificial Neural Network; CA, Cellular Automata; CENTROSUR, "Empresa Eléctrica Regional Centro Sur C.A."; D&H, Dalenius & Hodges; DER, Distributed Energy Resources; FoM, Figure-of-Merit; GIS, Geographical Information System; MAPE, Mean Absolute Percentage Error; MCDA, Multicriteria Decision Analysis; RMSE, Root Mean Square Error; SLF, Spatial Load Forecasting; TOPSIS, Technique for Order of Preference by Similarity to Ideal Solution; TR, Transition Rule; WLC, Weighted Linear Combination.

* Corresponding author at: Av. Max Ulhe y Pumapungo, CENTROSUR, 010209 Cuenca, Azuay, Ecuador.
E-mail address: sergiopza.24@gmail.com (S. Zambrano-Asanza).

https://doi.org/10.1016/j.ijepes.2022.108906
Received 1 December 2020; Received in revised form 1 October 2022; Accepted 15 December 2022
Available online 28 December 2022

Table 1
Summary of the main characteristics of previous works.

REF.	Pattern identification	Simulation method	Multi-class customers	Components in the model	Model validation	# Factors / Temporality
[7]	Data mining / Takagi–Sugeno fuzzy	–	Residential, Commercial, and small Industrial	(1) Preference patterns	–	8 / 1 year
[8]	Fuzzy inference model	Cellular Automata	Industrial, Domestic, Commercial	(1) Preference patterns, (2) neighborhood, (3) innovation factor as random noise	Spatial error	6 / 1 year
[9]	Analysis of risk factors	Cellular Automata	Farm, Industrial, Commercial, Residential	(1) Land-use change, (2) neighborhood	–	5 / 1 year
[10]	Evolutionary heuristic	Cellular Automata	Residential, Commercial, Industrial	(1) Preference patterns, (2) neighborhood	–	10 / 1 year
[11]	Evolutionary heuristic	Multi-Agent	Residential, Commercial, Industrial	(1) Preference patterns, (2) neighborhood and random, (3) non-natural new loads	Spatial error	10 / 1 year
[12]	Evolutionary heuristic	Power-law distribution with fractal exponent	–	(1) Preference patterns + stochastic factor, (2) neighborhood, (3) urban poles	Spatial error	10 / 1 year
[16]	–	Spatial Convolution	–	(1) Neighborhood	Spatial error	–
Proposal	Big Data / Artificial Neural Network	Cellular Automata	Residential, Commercial, Industrial	(1) Preference patterns, (2) neighborhood, (3) constraints, (4) stochastic factor	Spatial error pattern	11 factors + 8 constrains / 10 years

used to estimate the effective number of consumer growth based on potential for development and a global geographical trending controlling the development.

An analysis of the risk factors that influence urban load is studied in [9]; it was concluded that the land-use change and load density per unit area are the main factors. Then, using a GIS-based CA model, the load forecast is determined by analyzing the risk of change in land use and load density, demonstrating the feasibility of the method for a specific city.

A cellular automaton model for the spatiotemporal allocation of new loads is presented in [10]. An evolutionary heuristic calculates the probability of development, thus defining the probable preferences for each cell based on the similarity of its localization to other similar cells. A multi-agent system for SLF is proposed in [11] to simulate the different social dynamics involved in distribution networks. Two different parallel propagation algorithms are used in the simulation to consider natural and non-natural load growth. The same authors determine in [12] the future load density through a heterogeneous distribution using a power-law distribution with fractal exponent. There is an information interaction between two modules, one global and the other local, to characterize the load growth. A development suitability of the cells or preference map is estimated in [6] by binary regression through a generalized additive model.

The integration of artificial neural networks and cellular automata model (ANN-CA) with GIS has been used to simulate the evolution of land uses within urban growth models [13,14]. In order to consider several stages of development in the cells, [15] proposes the incorporation of the urban development theory expressed as an S-shaped curve. A transformation probability is used to update the state of each cell, derived from the historic dynamic process. This problem is solved with a gradient CA, showing greater precision in terms of spatial patterns and quantitative assessment indices.

A method based on two-dimensional spatial convolution is proposed in [16] to simulate the influence of the neighborhood in the load growth, which is controlled by a global prediction. As future works, the use of the S-shaped curve and pattern recognition with machine learning techniques is suggested.

Table 1 summarizes the main characteristics of the articles reviewed; the last row details the characteristics of this proposal presented in this paper. Columns 2 and 3 describe the methods used both for the identification of spatial patterns and the simulation itself. Most of the works have a global control of the load to be spatially distributed by the simulation method and use a multi-class analysis of consumers (column 4). The number of components in the model described in column 5 varies depending on the method and the detail of input information. The last two columns show the validation of the model and the details of the factors used.

1.2. Identified research gaps

According to the discussion above, there are research gaps that have not yet been completely addressed and others that need to be further studied, including:

- The development of the transport charging infrastructure, a spatial planning challenge, will increase the demand of the electricity network; therefore, allocation of capacity should be done from spatial information to reduce adverse impacts on the network [4].
- Generally, a CA model is calibrated only once in the base year to evolve in discrete steps of time [13,17]. Complex spatial–temporal models are necessary to effectively and timely establish solutions for urban changing dynamics [17]. Multiple dimensions require consideration, i.e., spatial and temporal, as well as horizontal and vertical growth. In order to determine where and how much a small area can be developed over time, those multiple dimensions should be reflected in the model's transition rules [17].
- The simulation models for long term load forecasting need to include mainly two dimensions using a higher geographic resolution in space and greater granularity in time [18].
- Spatial error has not been quantified in some methods for SLF [9–12,16]. The purpose of calculating an error metric in the SLF is to determine if the error contributes to poor planning of the distribution network expansion needs [5]. In this sense, in addition to measuring the error in magnitude, it is necessary to measure the spatial error, which identifies where and how these errors are located.
- It is necessary to take advantage of big data analytic to calibrate and validate integral frameworks, ranging from acquisition, geo-processing, spatial analysis to model development [19]. Thus, it is required to develop tools and models that facilitate the extraction of useful patterns or knowledge from large-scale data, so future actions could be predicted [20].

1.3. Contributions

To fill a good part of those gaps, this paper proposes a model for long-term spatial–temporal load forecasting through a simulation method of land use. A cellular automata method is adopted in this spatial simulation, which integrates artificial neural networks (ANNs) to estimate the

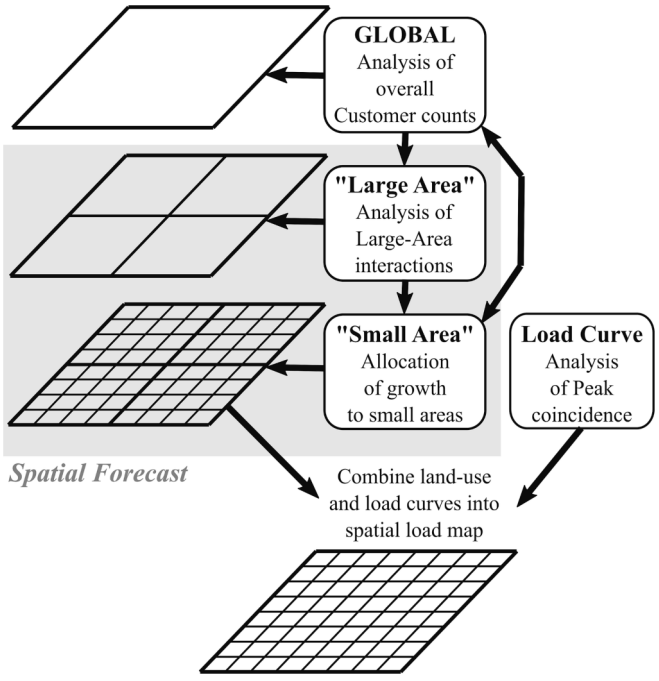

Fig. 1. Overall structure of a simulation method [5].

transition rules based on spatial factors that characterize land use development patterns. The state of each cell is determined by a probability of development associated with the land use preferences, the neighborhood effect, the constraint factors, and a stochastic disturbance. The ANN-CA simulation determines the number of future customers in small areas and in discrete time steps, which is controlled by a global forecast in large areas. At the end, a per capita consumption by consumer class is used to quantify electric load growth and allocation. For proper data management and comprehensive control of algorithm development and execution, a geospatial framework supported by Python tools is created. The main contributions of this work are:

- A development suitability or preference map is determined, as part of the transition rules of the spatial simulation method, through machine learning for the recognition and prediction of land-use patterns. An artificial neural network is trained using spatial criteria and considering temporality based on historical dynamics.
- The proposed framework adds temporality to the simulation with the constrained CA, both in the allocation of consumers by large areas (with the updating of states), and in the planning time stages until the long-term horizon year.
- Measurement of the spatial error pattern to validate and tune the performance of the model. It is proposed a loss function to validate the training and calibration of the ANN model. A second assessment uses a confusion matrix for the binary prediction task and validation metrics to calibrate the performance of the model.

2. Land use simulation for load forecasting

SLF methods fall into three categories: trending, simulation, and hybrid [5]. This work will focus on simulation methods, also known as geo-simulation when used within geographic environments. Through simulation, the planner tries to replicate the historical behavior in order to determine the future load growth; this includes spatial, temporal and magnitude information.

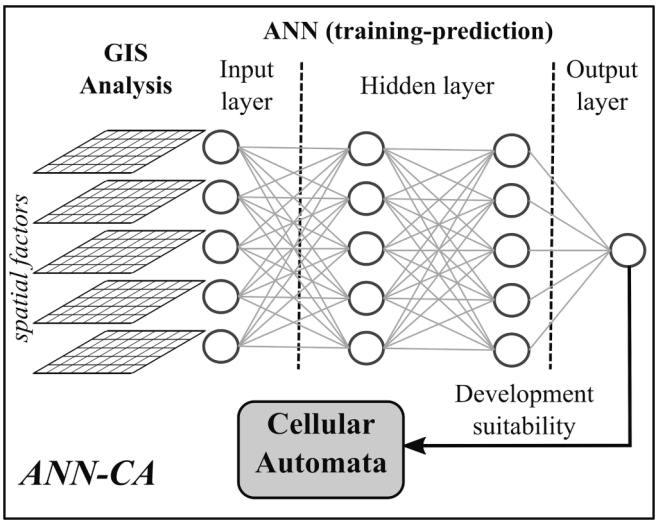

Fig. 2. Spatial forecast module using an ANN-CA model with GIS.

2.1. Top-down load forecasting

A top-down structure is generally adopted for simulation methods, as shown in Fig. 1 [5]. At the top is the global forecast and, through a series of steps, consumer growth is assigned to small areas, where spatial resolution is increased. The global load forecasting in large areas is well known by Electric Utilities, where time series regressions and trends analysis are used [21]. This forecast is done by consumer classes, which are assigned from large areas to small discrete ones using some type of land-use analysis [5]. Furthermore, a bottom-up approach adjusts the growth of demand for each small area to a previously defined total forecast, using per capita consumption for each consumer class.

2.2. Development in small areas

Most simulation methods use two modules [5]: 1) spatial consumer locations, and 2) temporal per capita consumption. The first module (Spatial Forecast in Fig. 1) is represented by the integration of ANN-CA using GIS, which is combined with end-use load curves of consumers to obtain the small area load forecast. The spatial allocation of consumer classes at the level of small areas and the land-use development depends on a location preference. The recognition of land-use development patterns is a powerful tool for determining future electric demand growth (how much, when, and where) [5].

There are usually two approaches to developing a location preference map: land use preferences [5,6] and similarity based on past observations [5]. Both approaches are used in this proposal. The first has been named as **development suitability**, obtained through the ANN model, while the second approach is addressed in the CA model in the sense of using the past development states of small areas through spatial convolution. The development suitability denotes the interest of a consumer to find a land space that meets the expectations of land use, obtained from spatial factor machine learning process, as shown in Fig. 2.

An ANN is organized by simple units interrelated in an extensive and parallel way, which allows modeling complex behaviors and patterns [22]. In Fig. 2, it can be seen that the ANN consist of a multi-layer perceptron with three main components: input layer, hidden layers, and output layer. Among its advantages are the use of different types and distributions of data, as well as solution of non-linear problems [13]; it also reduces subjectivity in the definition of rules and calibration of models.

Table 2
Spatial factors in the input layer of the ANN model.

Group	#	Spatial Factor
Local	1	Restrictions
(factors of the small area)	2	Slope
Proximity to	3	Main streets
	4	Shops
	5	Cultural spaces
	6	Schools
	7	Recreational places
	8	Health service
	9	Security services
	10	Downtown
	11	Industries
Surround	12	Customer density

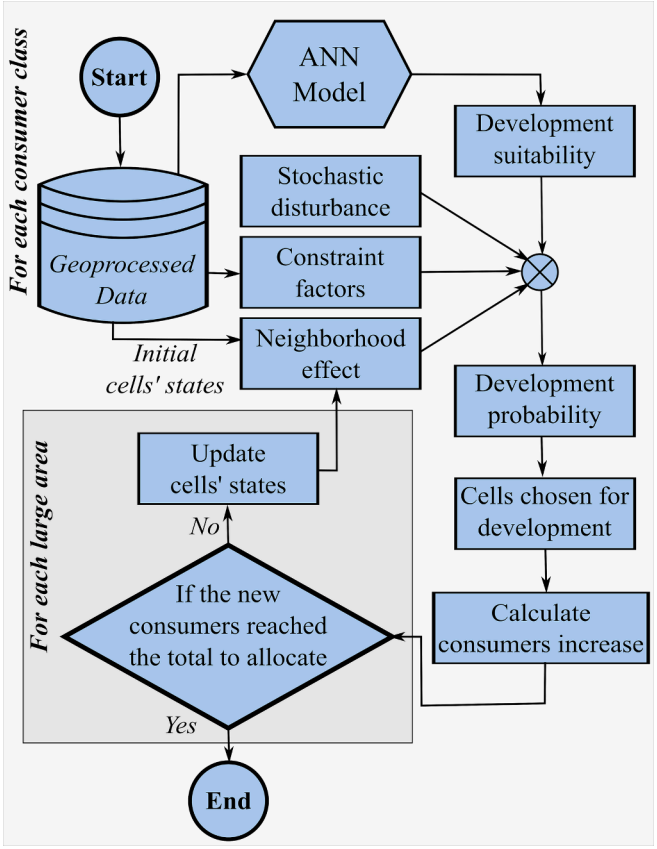

Fig. 3. Flowchart of the ANN-CA model.

2.3. Spatial factors

Each consumer class has specific location needs and each land-use class has characteristic attributes, which are called spatial factors or criteria and are classified as local, proximity, and surround [5]. Local factors are related to the land's suitability and its restrictions. Based on a function of distance, the proximity factors determine the level of influence. Moreover, surround factors measure influences by quantifying a magnitude within a neighborhood. The spatial factors detailed in Table 2 were chosen based on the availability and quality of information, as well as the representativeness of the study area.

The following spatial restrictions were used: protected land, watercourses, high landscape areas, higher slope areas, airports, parks, recreational areas, and military zones.

2.4. The ANN-CA process

The process begins with the preparation of the data in Fig. 3, which refers to the geospatial analysis of the factors, normalization, and preparation of formats, according to Algorithm 1. This input allows the supervised training and testing of the first ANN model with Algorithm 2, to later determine the development suitability of the initial year. With this result and adding the other terms of the formulation (e.g., stochastic disturbance, constraints factors, and the neighborhood effect as a function of the initial states) the land-use development probability is calculated.

Fig. 3 shows a flowchart to assign consumers to each large area. This iteration occurs in discrete steps of time in which cells are chosen to be developed based on the transition rules defined with the development probability and the given threshold value. In this process, the increase in consumers is calculated for each chosen cell, which depends on its location. Customer allocation ends if the expected total for each large area is reached. If this target is not yet reached, then the states of each cell are updated to reapply the neighborhood convolution and determine a new development probability, and then the process is repeated.

Algorithm 1. (*Geospatial analysis*)

```
Define global variables
Read geodatabase: vector format
Define functions:
  def spatial-factors-analysis
    for each year
      Calculate Euclidean distance, focal statistics, TIN slope, rasterizing and
convert them in an array
    end for
  return n-dimensional array
  def normalization
    Min-max / scaling
  return normalized array
  def create mask
    with constraint factors
  return mask array
Execute the analysis
Save the arrays in a compressed file
```

Algorithm 2. (*ANN model*)

```
Define global variables
Read n-dimensional array
Define sets for training and testing
Define model and parameters
for epoch in num_epochs
  for batch in batch generator
    step 1. clear the gradients
    step 2. compute the output (forward)
    step 3. compute the loss
    step 4. use loss to produce gradients (backward)
    step 5. use optimizer to take gradient step
  end for
end for
Compute error metrics
Save the model
```

In the process of Fig. 3, after choosing a cell to develop for a consumer class, it is necessary to assign an incremental number of consumers based on their location. In principle, a new consumer would be assigned per cell; however, if there is larger growth due to the influence of the neighborhood, then that value will be used. The load density map for the base year is an input data to the framework and SLF methods [5]. This map represents the characterization of the peak demand, at the level of load points (consumers class and street lighting) referenced in GIS [23,24]. With current advanced metering infrastructure deployment, load characterization has improved [25,26]; however, load research studies are still essential to establish temporary per capita

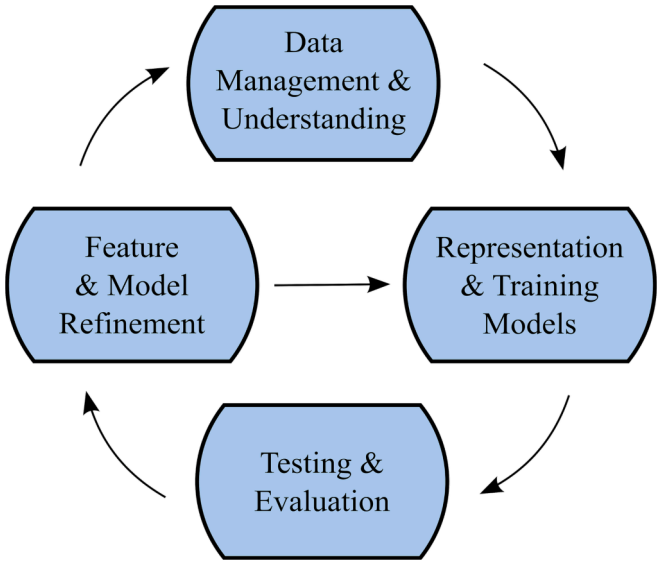

Fig. 4. Development cycle.

consumption and end-use load curves [27].

This process can be cyclical depending on the number of planning stages established in the long-term load forecasting, for example 3 stages every 5 years or an annual iterative process. Furthermore, at each planning stage there may be new hints that feed back into the process, such as new infrastructure projects, new highways, among others. In this way, the initially calibrated ANN model can be stored and reused or, failing that, continue learning. Thus, the load growth is determined for each consumer's class: Residential, Commercial, and Industrial.

2.5. Framework development cycle

For the construction and deployment of this comprehensive spatial–temporal load forecasting framework, the development cycle shown in Fig. 4 is proposed. An iterative process is carried out, from large-scale data management and understanding to model refinement, in order to meet the planner's needs and have a sophisticated forecasting tool. In general, the following activities are carried out at each stage:

- Data Management & Understanding: collect, understand, clean, prepare, structure and store data; geospatial processing.
- Representation & Training Models: feature representation; select algorithms; pick learning task; fit the estimator to the data.
- Testing & Evaluation: validate models; monitor outcomes; evaluate performance; compare alternatives.
- Feature & Model Refinement: sensitivity and tuning of the parameters; improve and optimize model; apply model to new data.

3. Method for spatial–temporal load forecasting

There are two well-known geo-simulation methods: CA and agent-based modeling [28]. In this work, a CA method is adopted for the spatial simulation. Transition rules play a fundamental role in generating spatial dynamics in CA models and many researchers have determined these rules from other models [29]. To determine the transition rules, a model based on ANNs is proposed here due to the robustness demonstrated in other areas of research [29].

3.1. Cellular automata

CA is a discrete simulation method that allows to model dynamic processes over time [28]. It has been widely used to find expansion patterns due to their ability to integrate spatial and temporal dimensions [15]. The proposed CA model is also called Constrained CA [29], since it is controlled by a macro-scale model. CA consists of the following components [28,29]: cells (raster-based GIS), states, neighborhoods (cells adjacent to the central cell), transition rules (TR), and discrete time steps. The state of cell k at time $t+1$ is a function of the state of the cell at time t, its neighborhood at t, and the transition rules [28], according to (1).

$$s_k^{t+1} = f\left(s_k^t, \Omega_k^t, TR\right) \quad (1).$$

where s_k^{t+1} and s_k^t are the cell states in which 1 corresponds to developed and 0 represents not-developed. Ω_k^t is the state in the neighborhood and spatial dynamics are represented by TR; the latter constitutes the core component of the model [29].

To consider variety and heterogeneity in the CA model, a probability function will be used to represent the development of customers in a given cell. The state of a cell k at time $t+1$ is defined in (2) according to land-use development probability P_k^{t+1}.

$$s_k^{t+1} = \begin{cases} 1, & if \quad P_k^{t+1} > \varphi^t \\ 0, & otherwise \end{cases} \quad (2).$$

where s_k^{t+1} is the cell state at time $t+1$ and φ^t is a threshold given at time t.

To extend this definition to a multi-class land-use simulation, each consumer class is represented by the index c: (R) Residential, (C) Commercial, and (I) Industrial. The development probability in (3) is mainly influenced by four factors [15,30]: the development suitability, the neighborhood effect, the constraint factors, and a stochastic disturbance.

$$P_k^{c,t+1} = Ps_k^{c,t} \bullet P\Omega_k^{c,t} \bullet P\chi_k \bullet P\varepsilon_k \quad (3).$$

where $P_k^{c,t+1}$ represents the land-use development probability of cell k for class c at time $t+1$, $Ps_k^{c,t}$ is the overall development suitability, $P\Omega_k^{c,t}$ refers to the neighborhood effect, $P\chi_k$ represents the constraint factors (being 0 = restricted, 1 = suitable), and $P\varepsilon_k$ considers the stochastic contribution typical of land-use development.

The neighborhood effect sets local transition rules based on the state of the cells immediately adjacent, which impacts the central cell [29]. In (4), a Moore Neighborhood type is proposed.

$$P\Omega_k^{c,t} = \frac{1}{\Omega - 1}\sum_j^{\Omega} s_j^{c,t} \quad (4).$$

where Ω is the neighborhood size (for example a rectangular neighborhood of 3x3) and $s_j^{c,t}$ is the state of the immediately adjacent cell j for class c at time t.

A stochastic term is incorporated into the model to generate plausible results with fractal properties [13], common in CA simulation. This can be defined by (5) and its distribution is highly skewed to values close to unity [31].

$$P\varepsilon_k = 1 + (-ln\gamma)^{\alpha} \quad (5).$$

where γ is a random number with a range from 0 to 1 and α is a parameter that controls stochastic disturbance with a constant value between 1 and 10 [15,30].

3.2. Development suitability

The development suitability, the first term in (3), is determined by training a backpropagation ANN. The location of future customer growth is related to spatial factors that drive development suitability. The objective is to define and calibrate a model that interprets these land-use development patterns based on historical dynamics [5,6]. Thus, the development suitability is represented in (6) as a function of n spatial factors.

$$Ps_k^{c,t} = f(x_1, x_2, \cdots, x_n) \quad (6).$$

where x_n is the nth spatial factor of cell k for class c and $f(x)$ is the fitting function that describes the probability of the development suitability.

Each spatial factor is associated with a neuron in the input layer; the output layer has a single neuron that represents the development

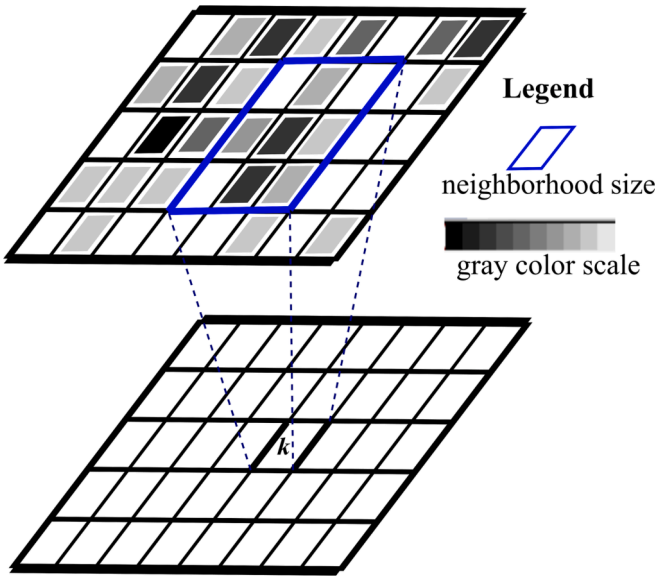

Fig. 5. Determination of the increase in customers and demand through spatial convolution.

suitability for each consumer class. It is convenient that the spatial factors are normalized in the range [0,1], so that they have the same importance. The signal received by each neuron in the hidden layers is calculated by (7) [13].

$net_{j,k}^{t} = \sum_l w_{l,j} x_{l,k}^{t}$(7).

where $net_{j,k}^{t}$ is the signal received by neuron j for cell k at time t, $w_{l,j}$ is the weight between layers from neuron l to neuron j, and $x_{l,k}^{t}$ is the lth spatial factor for cell k at time t. This last factor is associated with an activation function in each hidden layer.

Considering an output function of the sigmoid-type, and combining (6) and (7), the probability of development suitability is represented in (8).

$Ps_k^{c,t} = \sum_l w_{l,j} \frac{1}{1+e^{-net_{j,k}^{t}}}$(8).

where $Ps_k^{c,t}$ represents the probability of development suitability of cell k for class c at time t; $w_{l,j}$ is the weight between the last hidden layer and the output layer.

3.3. Incremental average of customers and demand

From the incremental number of customers per cell in the base year and using a spatial convolution of the Moore Neighborhood type (Fig. 5), the incremental average is determined in (9). The gray color scale in the upper map of Fig. 5 represents the incremental number of customers by consumer class, which is part of the geo-processed data.

$\widehat{\Delta L}_k^{c,t} = \frac{1}{\Omega'} \sum_j^{\Omega'} \Delta L_j^{c,t}$(9).

where $\widehat{\Delta L}_k^{c,t}$ is the incremental average number of customers of the cell k for class c at time t, Ω' is the neighborhood size, and $\Delta L_j^{c,t}$ is the incremental number of customers of the immediately adjacent cell j for class c at time t.

Analogously to the previous calculation, if the upper map in Fig. 5 represents the load density per cell (gray color scale), then the average demand is determined by (10) as a function of the neighborhood effect.

$\widehat{\Delta P}_k^{c,t} = \frac{1}{\Omega'} \sum_j^{\Omega'} \Delta P_j^{c,t}$(10).

where $\widehat{\Delta \boldsymbol{P}}_{\boldsymbol{k}}^{\boldsymbol{c,t}}$ is the average demand of the cell k for class c at time t, Ω' is the neighborhood size, and $\Delta \boldsymbol{P}_{\boldsymbol{j}}^{\boldsymbol{c,t}}$ is the demand of the immediately adjacent cell j for class c at time t.

Table 3
Confusion Matrix.

		Assigned **Positive**	*Cells* **Negative**
Actual Cells	**Positive**	True Positive (TP)	False Negative (FN)
	Negative	False Positive (FP)	True Negative (TN)

3.4. Model validation

As highlighted in the previous sections, global forecast and its distribution in large areas are assumed as inputs to the framework with a top-down approach to load allocation. At this level, the error in magnitude is important; however, in the spatial simulation, it should be adjusted to the total demand value of these areas. For this reason, this work will only measure the spatial error pattern, which is the most relevant at the micro-area level.

There are two types of validation in these models: the first one during the learning and training process of the ANN; and the second one at the end of the simulation process to calibrate the comprehensive performance of the model [32]. A first control measure is in the ANN-model calibration, according to Algorithm 2, at the backpropagation process during each epoch. In the forward step, a loss function is calculated; in the backward step, the gradient of the loss is used to update parameters [33]. Based on the testing data, the Mean Squared Error (MSE) loss function in (11) compares how far away the target prediction is; the lower this value, the better the model.

$Loss(y,\hat{y}) = \frac{1}{m}\sum_i (y-\hat{y})^2$(11).

where *Loss* is the MSE that averages the difference of the squares between predicted and objective values, y is a vector of m elements with the objective values, and $\hat{y}$ is a vector of m elements with the network's prediction.

The models for urban growth prediction, the closest to the SLF problem, are generally evaluated with overall accuracy and *kappa* index [22,32]. Since the CA model is a binary prediction for each consumer class, the second control measure uses a two-by-two confusion matrix shown in Table 3. On this basis, the accuracy (12) and F1-score (13) metrics will be calculated; the latter combines recall and precision into a single number.

$Accuracy = \frac{TP+TN}{TP+FN+FP+TN}$(12).

$F1\text{-}score = \frac{2 \cdot Recall \cdot Precision}{Recall+Precision} = \frac{2TP}{2TP+FP+FN}$(13).

Based on the same confusion matrix in Table 3, another widely used metric is the kappa index in (14) to measure reliability between two proportions.

$kappa = \frac{p_a - p_e}{1-p_e}$(14).

where p_a is the observed proportion of agreement (accuracy) and p_e is the proportion of agreement expected by chance [34].

When urban land-use changes are simulated, the previous indicators could overestimate the accuracy of the model for areas without changes [35]. The particularity of the SLF problem is that there is development both in vacant cells and in cells with an existing development because of the horizontal and vertical growth. The Figure-of-Merit (FoM) in (15) is another commonly used validation metric that excludes persistent simulation without changes from the accuracy calculation [15,30,35].

$FoM = \frac{B}{A+B+C+D}$(15).

where A is the number of cells developed but incorrectly determined without changes by the model, B are the cells developed that the model also observes as developed, C is the number of cells developed in a different class, and D is the number of cells without changes but the model incorrectly determines as developed.

4. Case study

The proposed approach was applied to the electrical system of the "Empresa Eléctrica Regional Centro Sur C.A." (CENTROSUR), located in

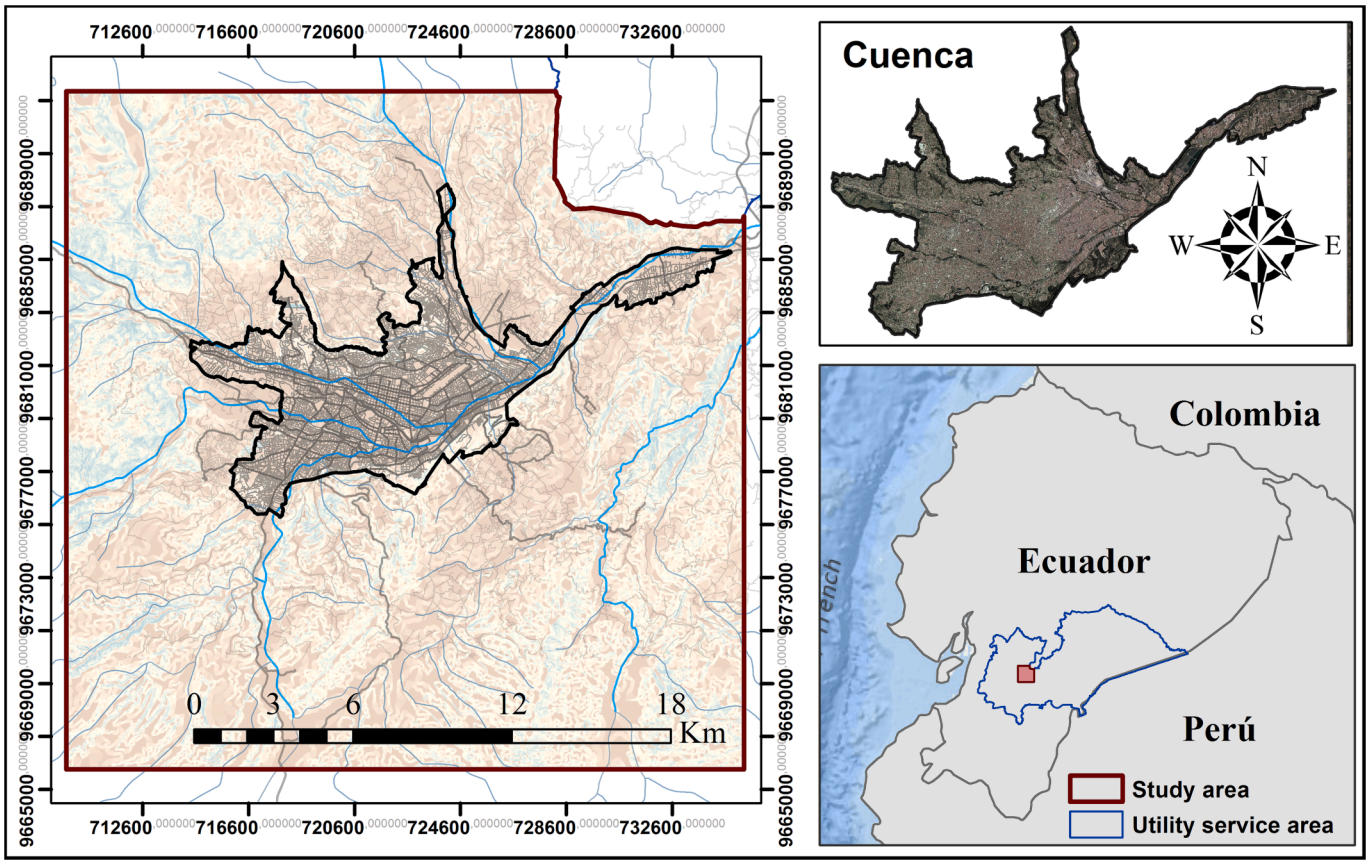

Fig. 6. Study Area of the Electric Distribution Utility, Cuenca – Ecuador.

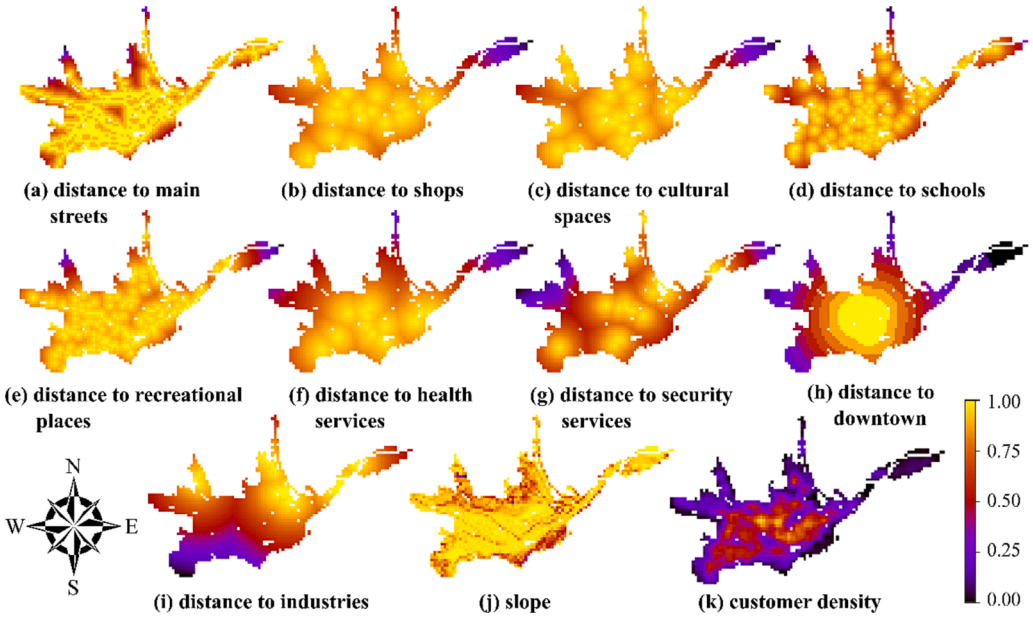

Fig. 7. Spatial factors of each cell used in the ANN model for residential class with 200 m x 200 m spatial resolution and min–max scaling.

Cuenca, Ecuador. The service area of CENTROSUR (Fig. 6) is 30,234 km^2 (11.8 % of Ecuadorian territory). The energy consumption of the 393,953 customers in 2018 (88 % residential, 11 % commercial, and 1 % industrial) was 1,074.10 GWh, with a peak demand of 194.93 MW.

The study area, colored in dark umber in Fig. 6, represents around 75 % of the Utility's energy demand. In this area, there are 214,082 consumers for the base year 2018. The upper right cut of the area corresponds to the border with another neighboring Utility.

4.1. Geo-processing of spatial factors

The software used to perform the GIS analysis was ArcGIS 10.6 from

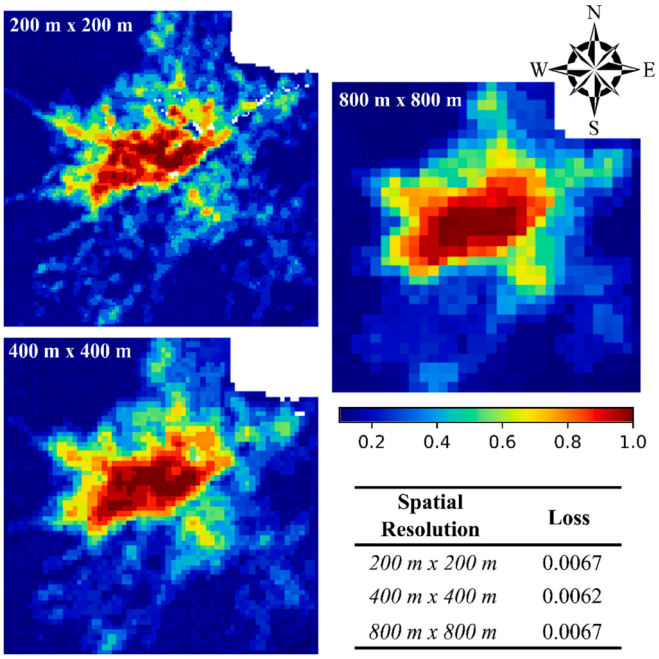

Spatial Resolution	Loss
200 m x 200 m	0.0067
400 m x 400 m	0.0062
800 m x 800 m	0.0067

Fig. 8. Suitability map for the residential class with D&H stratification and three spatial resolutions.

ESRI [36], and geo-processing was developed in Python with ArcPy package [37]. Three spatial resolution or cell size of raster data were used: 200 m, 400 m, and 800 m.

The spatial geo-processing of the factors is presented in Fig. 7. These criteria must be understandable and quantifiable [23]; thus proximity is a function of a Euclidean distance to small areas, the slope of the terrain is quantified as a function of degrees, and surround criterion is a function of a density or focal statistics within a neighborhood (Algorithm 1).

To determine the suitability score or preference map [6], it is important to normalize these criteria. Min-max scaling and Dalenius & Hodges (D&H) stratification [38] were used in Algorithm 1 with a range [0–1], where 1 is the most-desirable score, as observed in the heat maps in Fig. 7. For the purposes of a better visualization, the factors in Fig. 7 are displayed for the urban area of Cuenca but the following sections use the entire study area.

Generally, a base year is established to quantify these factors and obtain a development preference [5,6]. However, in this work, a 10-year time stamp was used to analyze factors to better calibrate the ANN training and the CA model. To store that spatial and temporal processing of large volumes of data in Python, an n-dimensional array was used in Algorithm 1. These arrays digitally capture the raster data of the geo-spatial and temporal analysis (from cells or micro-areas to rows and columns respectively), which facilitates the processing of mathematical models and underlying algorithms. The constraints are managed as a binary mask (0,1), where 0 represents the restricted areas, displayed as blank spaces in Fig. 7.

4.2. Suitability map

The spatial model forecasts where changes in land use occur, such as new development in vacant areas, redevelopment in existing areas, and reduced land-use density. For this purpose, a preference or suitability map is typically used for each consumer class in which a score is assigned to each small area to express a probability of change [5]. Then, an amount of change is allocated based on the highest scoring. The suitability map is the result of a supervised learning with the ANN model, where the features are given by the spatial factors and the target by the number of consumers in each cell.

Initially, the normalized data of factors and number of consumers per class are arranged considering several years for ANN training. This validation dataset was divided into 70 % for training and the remaining 30 % for testing. To structure a model according to the case study, three spatial resolutions were analyzed, as well as two techniques for normalizing spatial factors. To have a reference of an appropriate spatial resolution for the study area, 200 m were obtained for urban areas and 600 m for rural areas, as suggested in [39].

The suitability maps for the residential class are shown in Fig. 8 considering three spatial resolutions: 200 m, 400 m, and 800 m respectively. The loss value with the test data, after having trained the ANN, is reasonably good for each case (Loss $<$ 0.007). The heat map adequately describes the areas that have currently been developed (Fig. 8), highlighting that this development exceeds the urban limits of the city. Furthermore, Fig. 9 presents the results of the suitability maps for the commercial and industrial classes.

The processing time in the ANN model training using PyTorch [33] depends on the resolution and the number of epochs; however, an acceptable loss value is reached with 4,000 iterations. For example, adopting a resolution of 200 m (16,384 cells in the study area) and 3

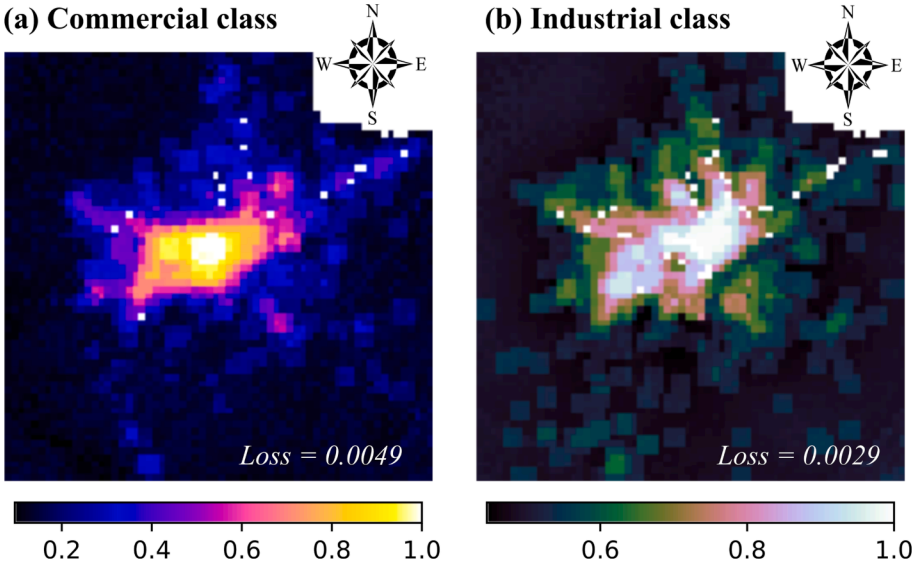

Fig. 9. Suitability map for commercial and industrial class with D&H stratification and 400 m × 400 m spatial resolution.

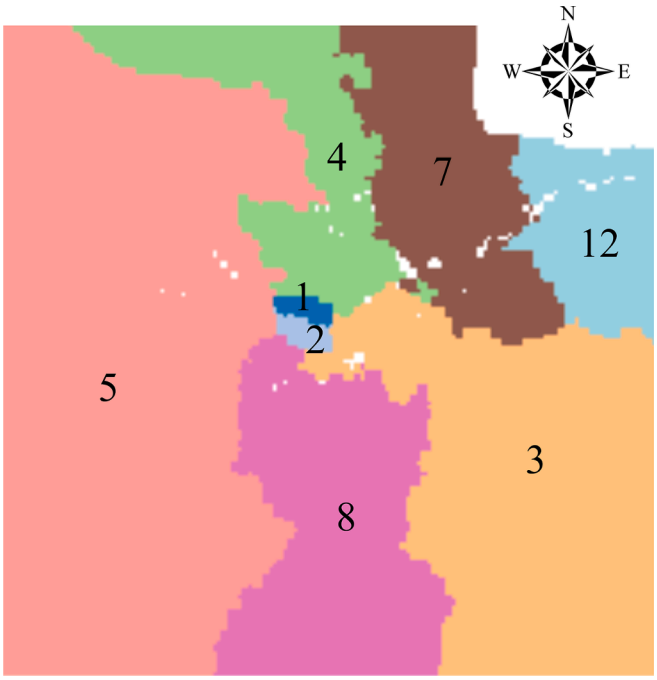

Fig. 10. Coverage of large areas of substations.

Table 4
Total customers of the base year to be assigned for each substation.

Substation	Residential	Commercial	Industrial	Total
1	77	60	1	**138**
2	54	66	1	**121**
3	725	178	3	**906**
4	763	135	11	**909**
5	1,814	372	15	**2,201**
7	612	132	4	**748**
8	562	108	1	**671**
12	150	54	1	**205**
Total	**4,757**	**1,105**	**37**	**5,899**

years of history for the 11 factors, the ANN training reaches losses below 0.007 within 2 min.

4.3. Calibrating the model

To calibrate the model and analyze the sensitivity of its parameters, the base information from the year 2018 is used. The large areas correspond to the coverage of eight substations that are within the study area (Fig. 10), obtained by the electrical connectivity of load points georeferenced in GIS. The number of new consumers per class to be assigned to each of these large areas is detailed in Table 4, with around 5,900 consumers in total. Two areas stand out, substations 1 and 2, which correspond to the historical center of the city with an underground network, where the growth of customers and load is lower than the others, since there is a high saturation. It is defined as objective the minimization of the error in the selection of cells to be developed, based on the knowledge of the cells that were developed in this base year.

As the spatial resolution increases, the error measurement is higher, so a comparison for different resolutions is not appropriate. Although using high spatial resolution in SLF carries more error, it is not necessarily a useless forecast [5]. In order to exemplify the measurement of the spatial error pattern, Fig. 11 shows the real distribution of residential class for the base year and the result of the simulation. The 4,757 consumers are distributed in 1,187 cells (400 m resolution), while the model selected 919 cells. The second row of Table 5 presents the spatial error

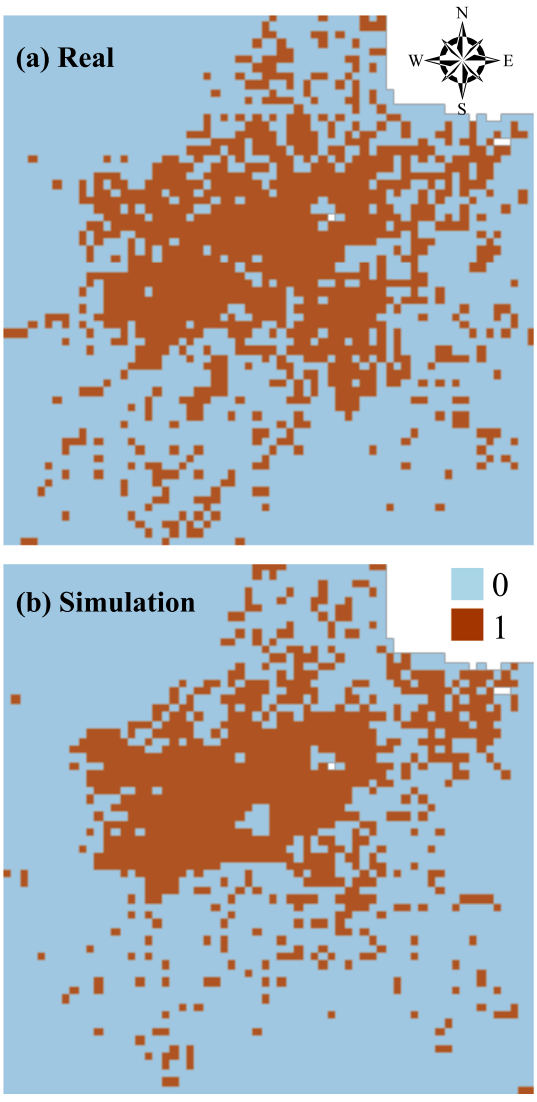

Fig. 11. Real distribution of residential class for the base year and the result of the simulation with 400 m × 400 m spatial resolution.

Table 5
Error metrics for two forms of normalization and different spatial resolutions.

Scaling	Cell (m)	Accuracy	F1-score	kappa	FoM
D&H	200	0.845	0.456	0.366	0.295
	400	**0.793**	**0.618**	**0.479**	**0.447**
	800	0.698	0.659	0.409	0.491
min–max	200	0.870	0.441	0.370	0.283
	400	0.776	0.483	0.370	0.318
	800	0.596	0.424	0.228	0.269

metrics obtained for this case.

Better handling of the data in the normalization task can improve error, as shown in Table 5. The first three rows use a D&H stratification, while the last three rows adopt the min–max scale. In general, the first normalization obtains the best indicators; furthermore, a resolution of 400 m is fairly acceptable in this study area.

The sensitivity and tuning of the rest of the parameters defined in the model were evaluated based on ranges of variation to find a suitable parameter in each case, according to the cycle described in Fig. 4. For example, parameter α in (5), which controls the stochastic disturbance and varies between 1 and 10, was set as 3. A threshold value $\varphi^t = 0.5$ was defined in (2) so that a cell with a higher development probability is

Table 6
Spatial error pattern metrics for all consumer classes.

Customer	Cell (m)	Accuracy	F1-score	kappa	FoM
R	200	0.845	0.456	0.366	0.295
C	200	0.932	0.312	0.286	0.191
I	200	0.998	0.000	0.000	0.000
Total	***200***	***0.855***	***0.416***	***0.342***	***0.266***
R	400	0.793	0.618	0.479	0.447
C	400	0.886	0.526	0.461	0.357
I	400	0.983	0.029	0.021	0.021
Total	***400***	***0.825***	***0.581***	***0.465***	***0.413***
R	800	0.698	0.659	0.409	0.491
C	800	0.832	0.632	0.526	0.462
I	800	0.938	0.118	0.086	0.062
Total	***800***	***0.754***	***0.624***	***0.430***	***0.462***

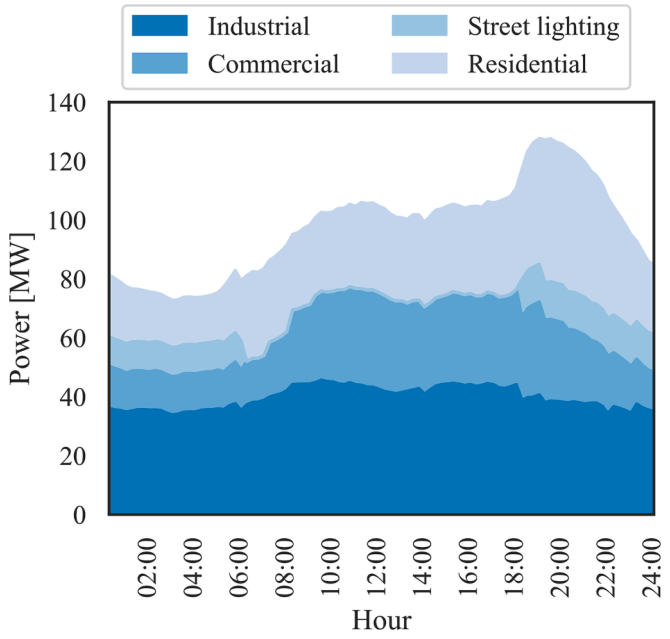

Fig. 12. Load curve by class of consumption for the day of peak demand of the base year.

chosen. Moreover, a rectangular neighborhood with a size of $\Omega = 3x3$ was established in (4) and it was found that a temporality of 3 years of history gave the best results.

Once it is established that the D&H stratification is the most appropriate, then the results are obtained for all classes of consumers. Table 6 summarizes the performance metrics of the model, where *Total* corresponds to a multiclass weighting based on the number of consumers to assign. If the number of consumers to be assigned is lower, the error will be greater, as can be seen with industrial consumers.

4.4. Input data for the SLF model

One of the main inputs for the SLF methods is the base year load density map [5], which quantifies the amount of demand in a small area. The planner mainly focuses on the day where the demand peak occurred, since the infrastructure must be planned to meet this requirement. Therefore, it is essential to characterize the load of the different classes of consumers and public lighting registered in GIS [40]. This laborious processing task is part of the bottom-up cycle in SLF methods [5]. A total of 271,269 load points, corresponding to residential, commercial, industrial consumers, as well as public lighting, are present in the study area.

The information measured by the SCADA system as well as smart meters at the consumer level was used, but the utility has not yet fully deployed this advanced metering infrastructure, so load research studies are still critical in this characterization task [27]. Considering the information provided by Electric Utility, Fig. 12 shows the load curve for 2018, whose shape is characteristic of residential consumption; the observed coincidence of peak demand occurs at 19:00.

The load density map for the base year is generated for 19:00 using a point density analysis, presented as a heat map in Fig. 13. As expected, high load densities are concentrated in the urban area of Cuenca city; however, there are certain urban clusters that are outside this limit. Furthermore, Fig. 13 also shows the spatially distributed load points in gray; as well as the service area of each substation in brown.

The calibration of the model was done using the coverage of eight current substations. For the analysis in these large areas (second block of the top-down structure of Fig. 1) the Electric Utility carries out a trend analysis to allocate the global load forecast. The Electric Distribution Utility uses Holt-Winters Exponential Smoothing technique for time series regression forecasting [41]. Well-known error measures such as MAPE (Mean Absolute Percentage Error) and RMSE (Root Mean Square Error) are used to validate this regression method [42,43]. The forecast of consumers and demand are presented in Fig. 14, where in each planning stage the forecast value is distributed for each substation with a trend analysis. For the demand time series, the MAPE is 1.51 %, while for the customers time series, the MAPE is 0.05 %. The Electric Utility has an annual cycle for updating this forecast.

The results of this analysis, disaggregated by consumer class and for three planning stages of 5 years, are presented in Table 7. It should be noted that these three planning stages were chosen in order to present a better visualization of the results. However, the proposed framework allows the use of a more granular planning cycle (annual example), even for a longer time horizon than the current one, according to the planner's requirements. This information constitutes the main input for the ANN-CA process detailed in previous sections.

To better explain the incremental value to be distributed from the total number of customers in the base year (Fig. 14), the total incremental value of the first planning stage (year 5 in Table 7) is added to obtain the total number of consumers of this last planning stage. This mathematical operation is: 214,082 + **28,049** = 242,131.

4.5. Results and discussion

This section presents the results obtained after the calibration of the model using the consumer class input data. To analyze the horizontal and vertical growth of consumers in each time stage, Fig. 15 presents a three-dimensional visualization of the study area. Moreover, the result of the demand growth for the long-term horizon year based on consumer growth is presented in Fig. 16. When comparing the load density of the horizon year with respect to the base year, it is possible to observe the development in certain areas by the variation of colors in the heat maps. Thus, to the west of the Cuenca city, within the urban limit, this development is mainly due to the construction of large apartments buildings. On the other hand, to the north, outside the urban limit, the growth is due to the construction of large urbanizations. The highest demand requirement according to the forecast is found in the service area of substation 5; since it is at the limit of capacity and physical space, it is necessary to plan a new substation.

As highlighted before, substations 1 and 2 have a lower value of customers and demand to distribute according to Table 7. From Fig. 15, it could be verified that for this urban area and cultural heritage, this growth is mainly vertical, due to the increase in trade, through changes from residential to commercial consumers. For this case, the second component of the CA method (neighborhood effect and loop in Fig. 3) characterizes this growth, since it is associated with the current and future state of each cell in its lifetime.

The demand for public lighting represents around 10 % of the coincident demand for the case study and its forecast is outside the scope

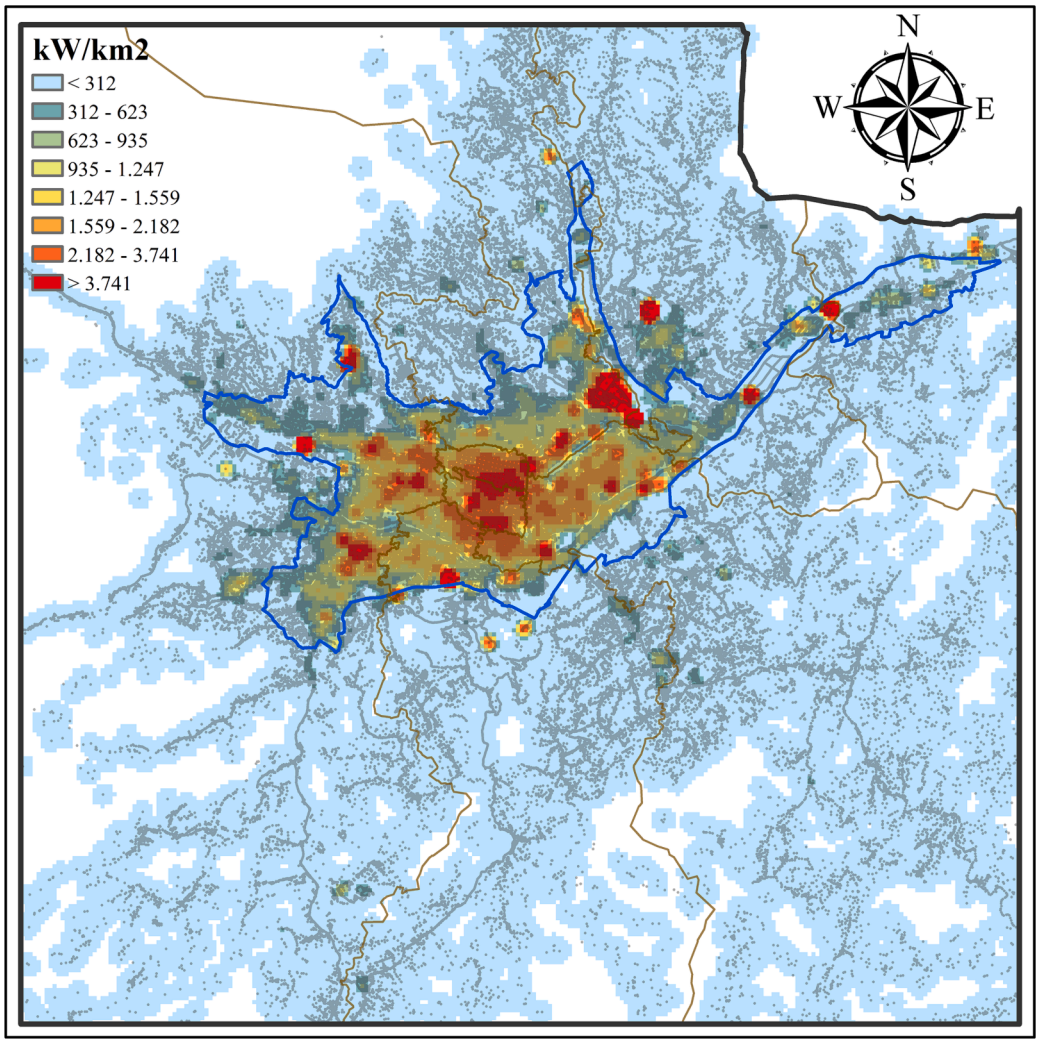

Fig. 13. Spatial demand density for the base year.

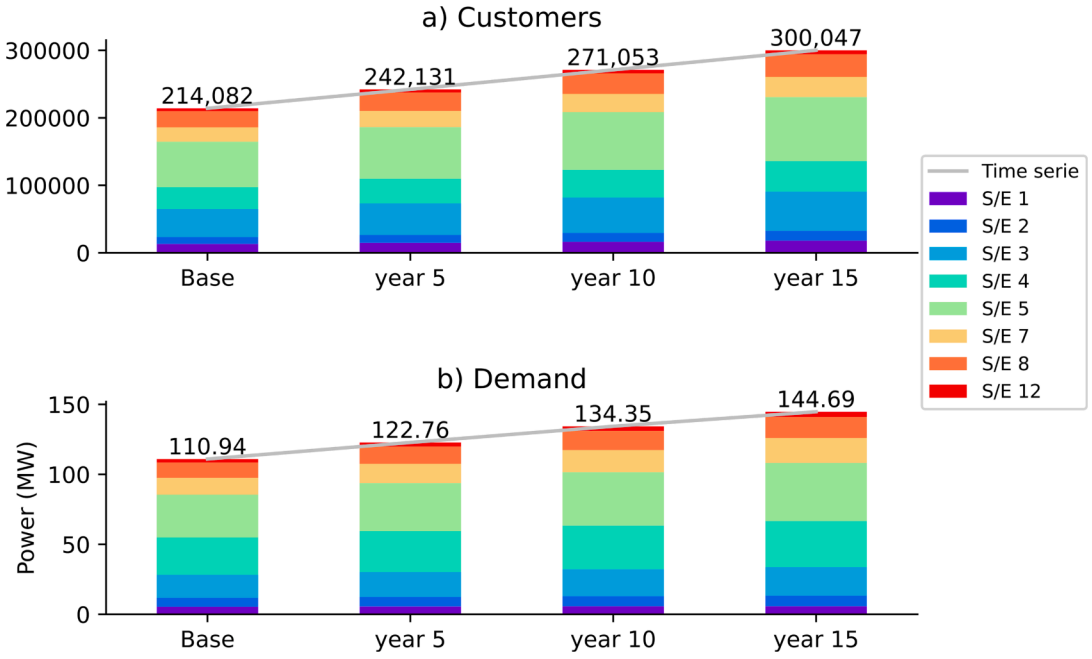

Fig. 14. Customers and Demand forecasting, distributed by substation.

Table 7
Incremental number of consumers and power for three planning stages.

		Customers (U)			Power (MW)		
Substation	**Class**	**Year 5**	**Year 10**	**Year 15**	**Year 5**	**Year 10**	**Year 15**
1	R	1,129	1,163	1,163	0.07	0.06	0.02
1	C	523	535	534	0.09	0.08	0.03
1	I	1	4	7	0.01	0.01	0.01
2	R	801	826	825	0.11	0.10	0.08
2	C	525	539	538	0.34	0.31	0.23
2	I	1	1	4	0.01	0.01	0.00
3	R	4,948	5,099	5,099	0.81	0.80	0.65
3	C	493	505	505	0.51	0.51	0.41
3	I	4	11	24	0.10	0.10	0.08
4	R	3,918	4,038	4,037	0.58	0.47	0.40
4	C	281	288	289	0.28	0.22	0.19
4	I	3	18	35	1.63	1.31	1.12
5	R	8,219	8,470	8,472	1.84	1.86	1.70
5	C	673	691	691	0.81	0.82	0.75
5	I	8	18	34	1.10	1.11	1.01
7	R	2,681	2,764	2,763	0.59	0.65	0.64
7	C	131	133	134	0.15	0.16	0.16
7	I	3	5	12	1.09	1.19	1.17
8	R	2,905	2,993	2,993	0.71	0.75	0.68
8	C	248	254	254	0.51	0.54	0.49
8	I	7	3	16	0.11	0.12	0.11
12	R	512	529	528	0.20	0.22	0.21
12	C	34	34	35	0.15	0.16	0.15
12	I	1	1	2	0.05	0.05	0.05
Total	R	25,113	25,882	25,880	4.91	4.90	4.38
Total	C	2,908	2,979	2,980	2.83	2.79	2.42
Total	I	28	61	134	4.08	3.88	3.55
		28,049	**28,922**	**28,994**	**11.83**	**11.58**	**10.36**

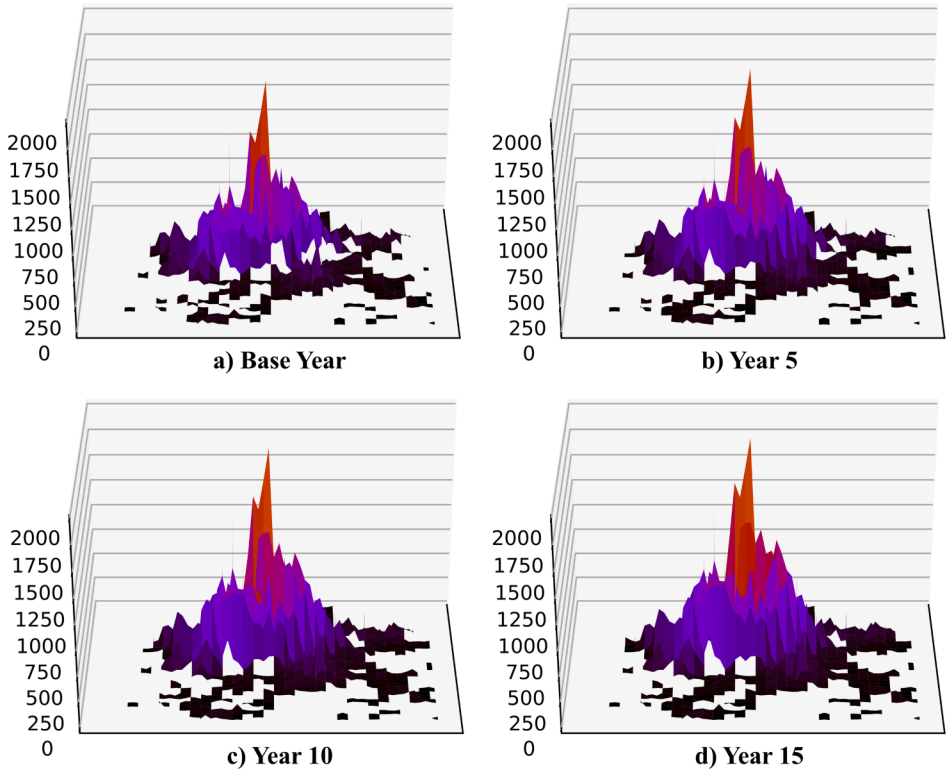

Fig. 15. Spatial-temporal growth of consumers during the planning stages.

of this paper. However, it has a correlation with the forecast results of residential consumers and other factors such as public roads, density or lighting levels, etc.

Renewable distributed energy resources (DER) are changing the shape of daily net electric loads in many regions, becoming the so-called "duck curve" [18]. DER penetration and active customer participation in demand response programs are becoming increasingly important, so utilities should implement more robust and comprehensive load forecasting models [18]. In this context, models must incorporate human decision behavior and preferences [24], which requires spatial and

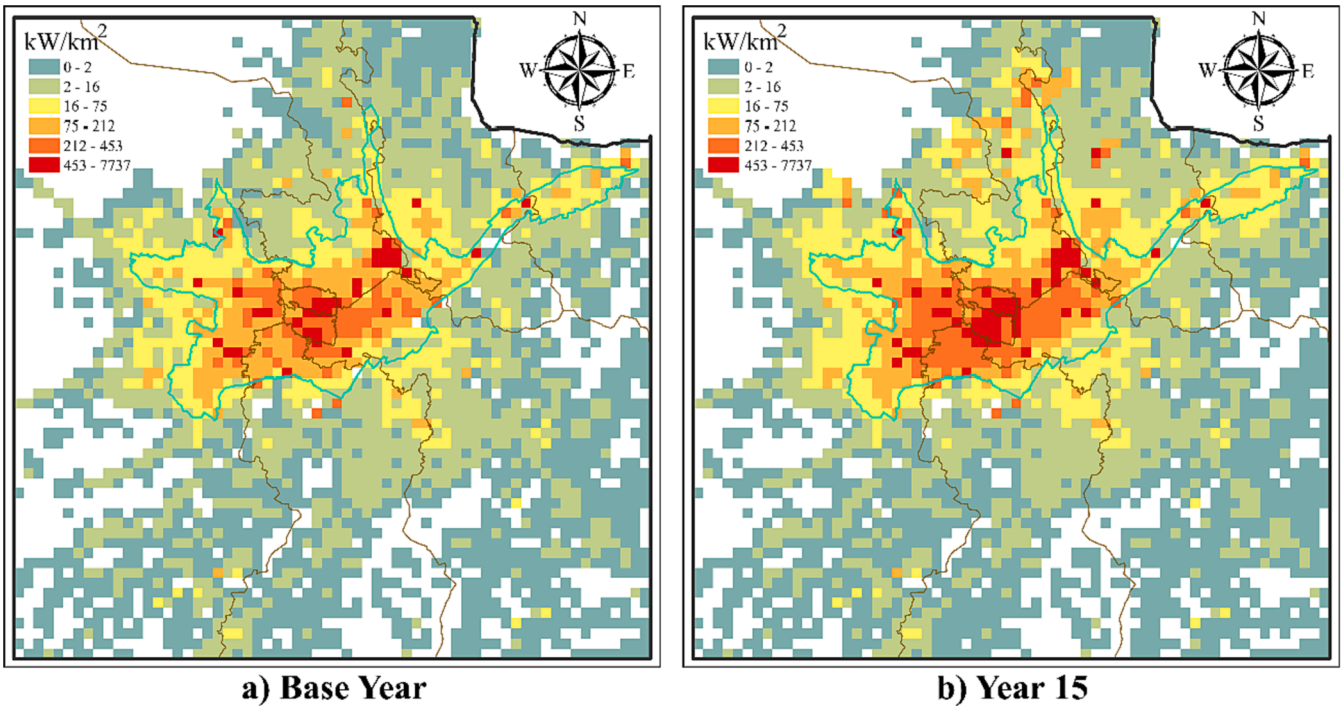

Fig. 16. Spatial-temporal load forecasting for the horizon year with 400 m × 400 m spatial resolution.

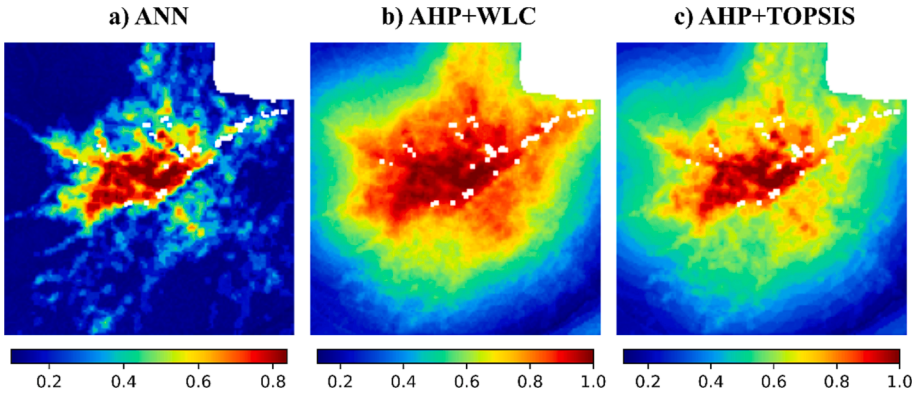

Fig. 17. Suitability map for the residential class with D&H stratification and spatial resolution of 200 m × 200 m, with three methods: a) ANN, b) AHP + WLC, and c) AHP + TOPSIS.

socioeconomic surveys on small scales. In the case study, a few consumers with photovoltaic solar microgeneration were observed, although not yet representative; however, it is crucial to begin characterizing this new prosumer class since it will significantly affect future decision planning.

In general, the diffusion of new end-use technologies, such as DER [2] or loads with high consumption [24], can be characterized as a new class, using the same essence of the proposed multi-class method. Until enough history is available to calibrate a model of development suitability and obtain adoption preferences, a good strategy could be correlation with other known technologies, such as induction cookers in the case study [24]. If, on the other hand, there is an important deployment of DERs, then the first step is to select the factors that would represent such adoption in each additional class, and then process the historical information. An example of such new classes is "Residential Rooftop Solar Photovoltaic", which could include storage, being part of self-consumption, net balance or a local energy market. Through innovation diffusion models and multiple scenarios, a forecast of large areas can be distributed to small areas using adoption maps [44], which can be done with a process similar to the proposed ANN-CA [45].

4.6. Comparison with other methods

The spatial dynamics represented by the transition rules constitute the core component of the suitability-based CA methods. Other modeling methodologies for these transition rules include the analytical hierarchy process (AHP), an approach of the multicriteria decision analysis (MCDA), Markov chain analysis, Fuzzy logic, and the SLEUTH model [29]. For comparative purposes, two well-known techniques that integrate GIS with MCDA will be used: Weighted Linear Combination (WLC), and Technique for Order of Preference by Similarity to Ideal Solution (TOPSIS) [28]. The weights of the factors of the case study have already been determined in previous works through an AHP procedure of comparison by pairs of decision makers [23,46].

In this comparison, the residential class with D&H stratification and spatial resolution of 200 m × 200 m are used. Fig. 17 shows the suitability map obtained with three methods: the proposed ANN, the AHP + WLC integration, and the AHP + TOPSIS integration. The ANN approach

Table 8
Spatial error pattern metrics for three spatial load forecasting methods and for the residential class with spatial resolution of 200 m × 200 m.

Method	Precision	Accuracy	F1-score	kappa	FoM
ANN-CA	0.434	0.845	0.456	0.366	0.295
AHP + WLC-CA	0.391	0.823	0.460	0.359	0.299
	(−9.9 %)	*(−2.6 %)*	*(0.9 %)*	*(−1.9 %)*	*(1.4 %)*
AHP + TOPSIS-CA	0.395	0.826	0.456	0.355	0.295
	(−9.0 %)	*(−2.2 %)*	*(0.0 %)*	*(−3.0 %)*	*(0.0 %)*

takes advantage of the temporal characteristics of the factors, with an automatic calibration of the model in the training phase. The other two MCDA methods take the weights and the factor information only from the year immediately prior to the base year 2018. Thus, the suitability map of the ANN visually presents a better representation of land use patterns.

The metrics of the spatial error pattern are quantified, integrating the three methods described with the CA simulation method, in order to assign clients and load in the substation areas. The details of the metrics are shown in Table 8; the higher the value for a given metric, the better it is the performance. The difference of the two methods in comparison to the ANN-CA approach is shown between parenthesis. In general, for the Precision, Accuracy and kappa indices, the proposal has better performance; on the other hand, for the F1-score and FoM indices, they are equal or close.

Fig. 18 shows the spatial error maps for the three methods, which consists of the difference between the real value of clients in the base year with respect to the spatial clients forecasting with each method. If the difference is negative, it means that the real value is lower than the forecast, which is represented with cold colors; on the other hand, if the difference is positive, it is represented with warmer colors. To the north of the city, a red point can be seen in all three methods, being the highest error value and corresponding to the horizontal growth of an urbanization.

5. Conclusions

A novel geo-simulation method to obtain the spatial–temporal load forecasting is proposed in this paper. The integration of an artificial neural network and cellular automata called ANN-CA model, determines the development of consumers and electric load in small areas, which is controlled by a global forecast in large areas. This development is associated with the land use preferences, the effect of neighborhood states, the spatial constraints, and a stochastic disturbance. The simulation process is multi-period depending on the number of states up to the long-term planning horizon, and is also multi-class, since it is evaluated for each consumeŕs class: Residential, Commercial, and Industrial.

A preference map by consumer class was determined through the training and tuning of an artificial neural network using spatial criteria and considering temporality based on historical dynamics. The prediction of land use patterns with machine learning are part of the transition rules of the CA simulation method. In this supervised learning process, better temporality features of the factors can be obtained through deep learning, such as a convolutional neural network architecture, which would be part of future research.

In this proposed framework, the temporal dimension was highlighted in two aspects: i) in the development of location preferences, mainly with land use preferences and the effect of neighborhood states, and ii) in the use of planning stages for the allocation of consumers by large areas. Regarding the first aspect, the probability of development changes over time due to the current state of small areas already developed (rapid growth or saturation according to the S-shaped curve) and the development of vacant areas. The second aspect has the flexibility of providing, at each planning stage, feedback to the process such as new infrastructure projects, new highways, among others.

A measurement of the spatial error pattern has been proposed to validate and tune the performance of the model, which has not been observed in previous publications. In the first part, the loss value obtained for training and calibration of the ANN model is quite acceptable (Loss < 0.007). Thus, it is possible to predict land use preferences by consumer class in small areas, where spatial factors have changed over time or where there are hints of important changes. The second part of the error assessment allowed the calibration of the integral performance of the model. Indicators that do not overestimate the accuracy of the model, such as F1-score, kappa, and FoM were used. In the case study, it was found that an adequate treatment in normalization and temporality for the factors, a neighborhood size, among others, lead to acceptable metrics (F1-score $= 0.581$, kappa $= 0.465$, FoM $= 0.413$) using spatial resolution of 400 m. A comparison with two suitability-based CA methods indicated that the proposed method is highly suitable for spatial load forecasting problems.

Utilities are beginning to use big data analytics strategies to add greater value to their processes, including load forecasting. The use of these tools (e.g., libraries in Python for geospatial analysis, machine learning, visualization, analytics, and data management) help to systematize an integral framework that goes from acquisition, geoprocessing, and spatial analysis to the development and calibration of models. This made it possible to obtain knowledge from large-scale data, add temporality to the model, use different spatial resolutions, and evaluate the sensitivity of parameters in very reasonable times. As well as it will help to have an integrated and granular load forecasting that incorporates the expected DER adoption.

In a future research work, an analysis based on growth scenarios could be carried out to consider penetration levels of new loads with high consumption and new classes of users that adopt DER. On the other hand, for better error control in this proposed constrained CA method, it

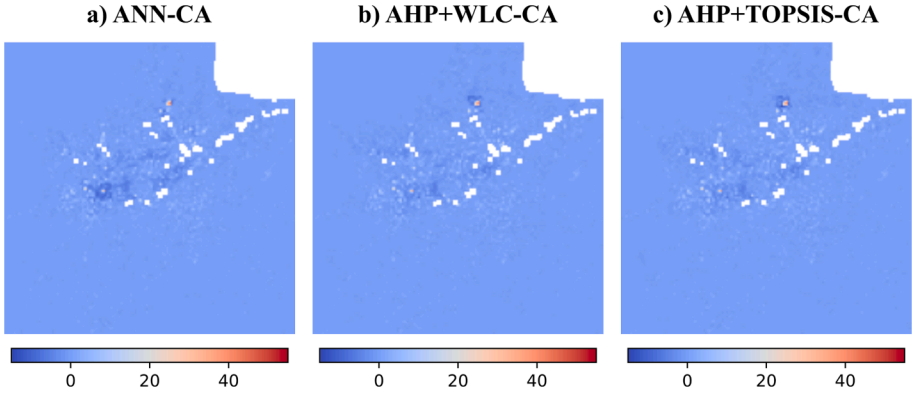

Fig. 18. Spatial error map for the residential class with spatial resolution of 200 m × 200 m, with three methods: a) ANN-CA, b) AHP + WLC-CA, and c) AHP + TOPSIS-CA.

can be complemented with hierarchical load forecasting in large areas. Thus, a hierarchical time series forecasting can be systematized under a spatial approach, which would be part of a future research.

CRediT authorship contribution statement

S. Zambrano-Asanza: Conceptualization, Methodology, Software, Validation, Formal analysis, Investigation, Resources, Data curation, Writing – original draft, Writing – review & editing, Visualization, Funding acquisition. **R.E. Morales:** Methodology, Software, Validation, Formal analysis, Investigation, Resources, Data curation. **Joel A. Montalvan:** Methodology, Software, Validation, Formal analysis, Investigation, Resources, Data curation. **John F. Franco:** Conceptualization, Validation, Formal analysis, Investigation, Writing – original draft, Writing – review & editing, Visualization, Supervision, Project administration, Funding acquisition.

Declaration of Competing Interest

The authors declare that they have no known competing financial interests or personal relationships that could have appeared to influence the work reported in this paper.

Data availability

The authors do not have permission to share data.

Acknowledgements

The authors would like to thank "Empresa Eléctrica Regional Centro Sur C.A.", Electric Distribution Utility of Ecuador, for the provided information and collaborative support.

This work was supported by the Brazilian institutions: Coordination for the Improvement of Higher Education Personnel (CAPES) - Finance Code 001, and the São Paulo Research Foundation (FAPESP), under grants 2015/21972-6 and 2017/02831-8.

References

[1] Sallam AA, Malik OP. Electric Distribution Systems. Hoboken, NJ, USA: John Wiley & Sons, Inc.; 2011. Doi: 10.1002/9780470943854.
[2] Heymann F, Silva J, Miranda V, Melo J, Soares FJ, Padilha-Feltrin A. Distribution network planning considering technology diffusion dynamics and spatial net-load behavior. Int J Electr Power Energy Syst 2019;106:254–65. https://doi.org/10.1016/j.ijepes.2018.10.006.
[3] Willis HL. Power Distribution Planning Reference Book. 2nd ed. Marcel Dekker; 2004.
[4] Jones R, Haley B, Kwok G, Hargreaves J, Williams J. Electrification and the future of electricity markets: Transitioning to a low-carbon energy system. IEEE Power Energy Mag 2018;16:79–89. https://doi.org/10.1109/MPE.2018.2823479.
[5] Willis HL. Spatial Electric Load Forecasting. 2nd ed. Marcel Dekker; 2002.
[6] Melo JD, Carreno EM, Padilha-Feltrin A. Estimation of a preference map of new consumers for spatial load forecasting simulation methods using a spatial analysis of points. Int J Electr Power Energy Syst 2015;67:299–305. https://doi.org/10.1016/j.ijepes.2014.11.023.
[7] Wu H-C, Lu C-N. A data mining approach for spatial modeling in small area load forecast. IEEE Trans Power Syst 2002;17:516–21. https://doi.org/10.1109/TPWRS.2002.1007927.
[8] Miranda V, Monteiro C. Fuzzy inference in spatial load forecasting. 2000 IEEE Power Eng Soc Conf Proc 2000;2:1063–8. Doi: 10.1109/PESW.2000.850087.
[9] He YX, Zhang JX, Xu Y, Gao Y, Xia T, He HY. Forecasting the urban power load in China based on the risk analysis of land-use change and load density. Int J Electr Power Energy Syst 2015;73:71–9. https://doi.org/10.1016/j.ijepes.2015.03.018.
[10] Carreno EM, Rocha RM, Padilha-Feltrin A. A cellular automaton approach to spatial electric load forecasting. IEEE Trans Power Syst 2011;26:532–40. https://doi.org/10.1109/TPWRS.2010.2061877.
[11] Melo JD, Carreno EM, Padilha-Feltrin A. Multi-agent simulation of urban social dynamics for spatial load forecasting. IEEE Trans Power Syst 2012;27:1870–8. https://doi.org/10.1109/TPWRS.2012.2190109.
[12] Melo JD, Carreno EM, Padilha-Feltrin A, Minussi CR. Grid-based simulation method for spatial electric load forecasting using power-law distribution with fractal exponent. Int Trans Electr Energy Syst 2016;26:1339–57. https://doi.org/10.1002/etep.2151.
[13] Li X, Yeh AGO. Neural-network-based cellular automata for simulating multiple land use changes using GIS. Int J Geogr Inf Sci 2002;16:323–43. https://doi.org/10.1080/13658810210137004.
[14] Aarthi AD, Gnanappazham L. Urban growth prediction using neural network coupled agents-based Cellular Automata model for Sriperumbudur Taluk, Tamil Nadu, India. Egypt J Remote Sens Sp Sci 2018;21:353–62. https://doi.org/10.1016/j.ejrs.2017.12.004.
[15] Liu X, Hu G, Ai B, Li X, Tian G, Chen Y, et al. Simulating urban dynamics in China using a gradient cellular automata model based on S-shaped curve evolution characteristics. Int J Geogr Inf Sci 2018;32:73–101. https://doi.org/10.1080/13658816.2017.1376065.
[16] Vieira DAG, Silva BE, Menezes TV, Lisboa AC. Large scale spatial electric load forecasting framework based on spatial convolution. Int J Electr Power Energy Syst 2020;117.. https://doi.org/10.1016/j.ijepes.2019.105582.
[17] Liu Y, Batty M, Wang S, Corcoran J. Modelling urban change with cellular automata: Contemporary issues and future research directions. Prog Hum Geogr 2019:030913251989530. Doi: 10.1177/0309132519895305.
[18] EPRI. Developing a Framework for Integrated Energy Network Planning (IEN-P). Palo Alto, CA: 2018.
[19] Stimmel CL. Big Data Analytics Strategies for the Smart Grid. 1st ed. CRC Press; 2015.
[20] Zobaa AF, Bihl TJ. Big Data Analytics in Future Power Systems. 1st ed. CRC Press; 2018. Doi: 10.1201/9781315105499.
[21] Lee WJ, Hong J. A hybrid dynamic and fuzzy time series model for mid-term power load forecasting. Int J Electr Power Energy Syst 2015;64:1057–62. https://doi.org/10.1016/j.ijepes.2014.08.006.
[22] Grekousis G. Artificial neural networks and deep learning in urban geography: A systematic review and meta-analysis. Comput Environ Urban Syst 2019;74:244–56. https://doi.org/10.1016/j.compenvurbsys.2018.10.008.
[23] Zambrano S, Molina M, Chumbi W, Patiño C. Modelo de Simulación Jerárquico para la Proyección Espacio Temporal de la Demanda Eléctrica: caso de estudio en CENTROSUR. Rev Técnica Energía 2018:7–16. https://doi.org/10.37116/REVISTAENERGIA.V14.N1.2018.91.
[24] Mejia MA, Melo JD, Zambrano-Asanza S, Padilha-Feltrin A. Spatial-temporal growth model to estimate the adoption of new end-use electric technologies encouraged by energy-efficiency programs. Energy 2020;191:116531. https://doi.org/10.1016/j.energy.2019.116531.
[25] Quilumba FL, Lee WJ, Huang H, Wang DY, Szabados RL. Using smart meter data to improve the accuracy of intraday load forecasting considering customer behavior similarities. IEEE Trans Smart Grid 2015;6:911–8. https://doi.org/10.1109/TSG.2014.2364233.
[26] Ye CJ, Ding Y, Wang P, Lin ZZ. A Data Driven Bottom-up Approach for Spatial and Temporal Electric Load Forecasting. IEEE Trans Power Syst 2019:1–1. Doi: 10.1109/tpwrs.2018.2889995.
[27] Puckett C, Williamson C, Godin C, Gifford W, Farland J, Laing T, et al. Utility Load Research: The Future of Load Research Is Now. IEEE Power Energy Mag 2020;18:61–70. https://doi.org/10.1109/MPE.2020.2972668.
[28] Malczewski J, Rinner C. Multicriteria Decision Analysis in Geographic Information Science. Berlin, Heidelberg: Springer Berlin Heidelberg; 2015. Doi: 10.1007/978-3-540-74757-4.
[29] Liu Y. Modelling Urban Development with Geographical Information Systems and Cellular Automata. London, England: CRC Press; 2009.
[30] Yao Y, Liu X, Li X, Liu P, Hong Y, Zhang Y, et al. Simulating urban land-use changes at a large scale by integrating dynamic land parcel subdivision and vector-based cellular automata. Int J Geogr Inf Sci 2017;31:2452–79. https://doi.org/10.1080/13658816.2017.1360494.
[31] White R, Engelen G. Cellular Automata and Fractal Urban Form: A Cellular Modelling Approach to the Evolution of Urban Land-Use Patterns. Environ Plan A Econ Sp 1993;25:1175–99. https://doi.org/10.1068/a251175.
[32] Aburas MM, Ahamad MSS, Omar NQ. Spatio-temporal simulation and prediction of land-use change using conventional and machine learning models: a review. Environ Monit Assess 2019;191:1–28. https://doi.org/10.1007/s10661-019-7330-6.
[33] Rao D, McMahan B. Natural Language Processing with PyTorch. O'Reilly Media, Inc.; 2019.
[34] Sim J, Wright CC. The kappa statistic in reliability studies: Use, interpretation, and sample size requirements. Phys Ther 2005;85:257–68. https://doi.org/10.1093/ptj/85.3.257.
[35] Chen Y, Liu X, Li X. Calibrating a Land Parcel Cellular Automaton (LP-CA) for urban growth simulation based on ensemble learning. Int J Geogr Inf Sci 2017;31:2480–504. https://doi.org/10.1080/13658816.2017.1367004.
[36] ESRI. ArcGIS: The mapping and analytics platform 2019. https://www.esri.com/en-us/home (accessed April 24, 2019).
[37] Toms S, O'Beirne D. ArcPy and ArcGIS - Automating ArcGIS for Desktop and ArcGIS Online with Python. 2nd ed. Birmingham, UK.: Packt Publishing; 2017.
[38] Dalenius T, Hodges Jr JL. Minimum Variance Stratification. J Am Stat Assoc 1959;54:88–101. https://doi.org/10.1080/01621459.1959.10501501.
[39] Melo JD, Carreno EM, Calviño A, Padilha-Feltrin A. Determining spatial resolution in spatial load forecasting using a grid-based model. Electr Power Syst Res 2014;111:177–84. https://doi.org/10.1016/j.epsr.2014.02.019.
[40] Zambrano-Asanza S, Molina M. Research and Characterization of the Load: Random Sampling by Strata. Cuenca, Ecuador: Planning Department Report - CENTROSUR C.A; 2016.
[41] Zambrano-Asanza S, Patino A. Proyección de la Demanda a corto, mediano y largo plazo. Cuenca, Ecuador: Planning Department Report - CENTROSUR C.A; 2021.

[42] Chen MR, Zeng GQ, Di LK, Weng J. A Two-Layer Nonlinear Combination Method for Short-Term Wind Speed Prediction Based on ELM, ENN, and LSTM. IEEE Internet Things J 2019;6:6997–7010. https://doi.org/10.1109/JIOT.2019.2913176.

[43] Zhao F, Zeng GQ, Di LK. EnLSTM-WPEO: Short-term traffic flow prediction by ensemble LSTM, NNCT weight integration, and population extremal optimization. IEEE Trans Veh Technol 2020;69:101–13. https://doi.org/10.1109/TVT.2019.2952605.

[44] Marcochi de Melo D, Villavicencio Gastelu J, Asano PTL, Melo JD. Spatiotemporal estimation of photovoltaic system adopters using fuzzy logic. Renew. Energy 2022;181:1188–96. https://doi.org/10.1016/J.RENENE.2021.09.113.

[45] Alderete Peralta A, Balta-Ozkan N, Longhurst P. Spatio-temporal modelling of solar photovoltaic adoption: An integrated neural networks and agent-based modelling approach. Appl Energy 2022;305:117949. https://doi.org/10.1016/J.APENERGY.2021.117949.

[46] Zambrano-Asanza S, Chumbi WE, Franco JF, Padilha-Feltrin A. Multicriteria Decision Analysis in Geographic Information Systems for Identifying Ideal Locations for New Substations. J Control Autom Electr Syst 2021.1305–16.;2021(325):32. https://doi.org/10.1007/S40313-021-00738-5.